Verification of nondimensional energy spectrum-based blast design for reinforced concrete members through actual blast tests

Huang, Zhiwei; Li, Bing; Lim, Chee Leong

2010

Li, B., Huang, Z., & Lim, C. L. (2010). Verification of nondimensional energy spectrum-based blast design for reinforced concrete members through actual blast tests. Journal of structural engineering, 136(6), 627–636.

https://hdl.handle.net/10356/95517

https://doi.org/10.1061/(ASCE)ST.1943-541X.0000149

Verification of Nondimensional Energy Spectrum-Based Blast Design for Reinforced Concrete Members through Actual Blast Tests

***Bing Li*[1]; *Zhi Wei Huang*[2]; *and Chee Leong Lim*[3]**

[1]*Associate Professor, School of Civil and Environmental Engineering, Nanyang Technological Univ., Singapore 639798, Singapore*

E-mail: cbli@ntu.edu.sg

[2]*Senior Engineer, J.P. Kenny Pty Ltd, Middlesex TW18 3DT, U.K.*

E-mail: Zhiwei.Huang@jpkenny.com

[3]*Research Fellow, School of Civil and Environmental Engineering, Nanyang Technological Univ., Singapore 639798, Singapore.*

E-mail: CheeLeong@ntu.edu.sg

Abstract:

A method has been developed for the design of reinforced concrete (RC) members when subjected to blast loadings based on the nondimensional energy spectrum. Numerical analyzes showed good agreement between the approximate responses of RC members designed to their respective levels of target response. This paper further verifies this method through the actual response of a RC column and beam subjected an actual denotation of explosives at a short standoff. When subjected to blast loading from a short standoff distance, the cantilever column behaved predominantly in direct shear. Thus, ways to mitigate the damage of a cantilever column should draw focus on the robustness. The developed design procedure provides a feasible method for the blast resistant design of members, subjected to blast loads at a short standoff distance.

CE Database subject headings:

Blast loads; Reinforced concrete; Numerical analysis.

Author keywords:

Blast load; Blast-resistant design; Reinforced concrete; Nondimensional energy spectrum.

Introduction

From observations of buildings subjected to deliberate or accidental blast loads at a short standoff distance, it can be seen that the collapse of the structural systems are due mainly to the failure of one or more critical structural members (Longinow and Mnizsweski 1996; Li et al. 2009; Luccioni et al. 2004). The result of the failure of a critical structural member is the redistribution of the internal forces within the structural system. If the increased demand resulting from the redistribution exceeds the capacity of the remaining members, subsequent failure of the remaining members may arise. This may result in an eventual failure of the structural system. Known cases of failure of structural systems include the Ronan Point Building and the Murrah Federal Building (Corley et al. 1998; Hinman and Hammond 1997; Mlakar et al. 1998; Hayes et al. 2005).

In recent years, a number of methods have been proposed for blast resistant design of reinforced concrete (RC) members (ASCE 1985; Allgood and Swihart 1970; Biggs 1964; TM5- 855-1, United States Department of Army 1965; May and Smith (1995). These are based on the performance of the RC members with an explicit consideration of the behavior of the member beyond its elastic region of response. The focus of these design methods ensures that the performance of the designed members contributes toward the safety of the structure. In a performance-based design framework for structures subjected to blast loads, it is common to select appropriate response parameters as performance indicators of the members. Using these selected parameters, the expected performance level can be established and applied to the design in limiting the extent of the response and the damage level of the member. Currently, two performance indicators which are commonly used are: (a) the target support rotation of the member (TM5-1300, United States Department of Army 1990; May and Smith 1995) or (b) the target displacement ductility factor expected of the member (TM5-855-1, United States Department of Army 1965; Biggs 1964; Manual 42, ASCE 1985). The target support rotation refers to the rotation at the support of an equivalent single-degree-of-freedom system, which represents the structure. Given a target support rotation y_t or a target displacement ductility ratio μ_t for a critical location along the span of the member to be designed (e.g., the midspan of a simply supported member or the free end of a cantilever member), the blast design can then be carried out.

However, research pointed out that neither y_t (i.e., target support rotation) nor μ_t (i.e., a target displacement ductility ratio) alone could provide a complete definition of the performance of a structural member under blast loads (Rong and Li 2008). In other words, design for blast resistance should in effect consider both the target support rotation and the target displacement ductility. Such a method for the design of RC members for blast resistance has been developed, which is based on nondimensional energy spectrum (NES). Numerical analyses show good agreements between the approximate responses of RC members designed to their respective levels of target responses. This was demonstrated using equivalent single-degree-of-freedom systems. While the approximate responses of the RC members were shown to be lower than the target levels of response, this difference is considered to be conservative and leaves a buffer for additional response of the member. Since this was based on numerical analyses, the study now verifies the feasibility of the design method through the actual response of a RC column and beam subjected to blast loads arising from the physical detonation of explosives at a short standoff distance. This was conducted under the support of Defense Science and Technology Agency, Singapore.

The main objectives of this study are as follows:

1. To understand the behavior of RC columns and beams, which are designed with the method developed based on NES, when subjected to blast loads at a short standoff distance. The RC members have been designed according to the target levels of response expected of such a blast load. From this, it is hoped that a better understanding of the behavior can provide certain insights in mitigating

damage of RC column and beams due to blast loads at a short standoff distance.

2. To compare the actual distributions of pressure as recorded during the blast load with the approximate values from a widely used program such as CONWEP (Hyde 1991).
3. To determine the displacement responses of the RC members under the blast loads, which were designed by the NES method, by carrying out a double integration on the time history of acceleration as recorded, with respect to time. An approach for the processing of the data was undertaken to remove the noise content.
4. To compare the displacement responses as determined with the corresponding target values employed in the design.
5. To verify the feasibility of the design method based on NES by ascertaining whether it produces a viable design for a blast scenario at a short standoff distance. This verification will be based on observations from explosion testing of a RC column and RC beam, which may include phenomena that cannot be adequately captured by numerical analyzes.

Blast Design Based on NES

A blast resistant design procedure was proposed based on NES (Rong and Li 2008). The method first establishes a target level of response for an RC member subjected to blast loads, which considers both the target support rotation and the target displacement ductility of the RC member. With a primary set of design parameters such as member dimensions, material properties and also reinforcement amounts, the designer then approximates the maximum displacement and displacement ductility ratios of an equivalent single-degree-of-freedom (SDOF) system. The design parameters include the following: (a) the effective depth *d*, (b) the longitudinal reinforcement ratio ρ_h, and (c) the transverse reinforcement ratio ρ_v. As there will be differences in the target response of the RC member and the approximate response of the SDOF system, an iterative process is undertaken to revise the design parameters.

A structural member with continuous mass and stiffness can be represented by an equivalent elastic-plastic SDOF system with an equivalent mass and stiffness. The equivalent SDOF system is such that the deformation response of the concentrated mass is assumed to be the same as that for the critical point on the structural member (e.g., the midspan of a member with two ends constrained or the free end of a cantilever member). Due to the complicated behaviors of continuous RC members, some differences between the responses of the equivalent SDOF system and those of the designed member are conceivable (Fig. 1). Thus, the responses of the equivalent SDOF system under a given blast loading should achieve the expected performance level defined by y_t and μ_t. To achieve this objective, there exists only one solution in the form of the initial stiffness (k_e) and ultimate strength (R_m) for the equivalent system. Therefore, it is clear with the condition $y_e=y_t/\mu_t$ having satisfied, and the maximum displacement response of the equivalent SDOF system k_e having reached y_t exactly, the maximum displacements of equivalent systems with initial stiffness are either larger or smaller than k_e but not equal to y_t. The specific solution for k_e and R_m of the equivalent SDOF system can then be obtained by an iterative procedure. Assuming an initial stiffness k_e, parameters of the system are obtained and then additional design parameters are found by referring to the NES curves.

The iterative process seeks to revise the design parameters such that the approximate responses are similar to the corresponding target responses. During the iterative process, the difference between the target response and the approximate response was determined and design parameters were revised to minimize this difference. Details of this design method are described by Rong and Li (2008).

Experimental Studies

The design method seeks to vary the design parameters of the RC member such that the displacement and displacement ductility of the RC member is similar to the target responses. By doing so, the design would satisfy the expected performance of the RC member for a given blast load. However, assumptions were made during the design process, which include the following:

1. The behavior of the RC member will be predominantly in flexure; any possible shear failure will be precluded by sufficient shear reinforcement;
2. The response of the RC members can be approximated using an equivalent SDOF system;
3. The approximation of the second moments of inertia and flexural capacities is reasonably accurate for a nonhomogenous material such as concrete; and
4. The design parameters under the blast conditions are accurately defined. These parameters include the following: (a) the peak reflected overpressure P_r; (b) the duration of the positive phase t_d; and (c) positive phase reflected impulse I_r.

For a RC member subjected to blast loads, any discrepancies between these assumptions and reality, would lead to a corresponding difference between the actual response and the target response. In order to test the design method as developed (Rong and Li 2008), it becomes necessary to derive observations by subjecting RC members to actual blast loads. The observations from one RC column and one RC beam shall be discussed in this paper. The details about this explosion testing are given in the following sections.

Design of Specimens

A cantilever RC column and simply supported RC beam were designed by adopting the NES based design method. The schematic diagram of the column is shown in Fig. 2. The RC column and beam were designed to resist the blast load produced by the detonation of 100-kg TNT or equivalent, with standoff distances of 5 and 6 m, respectively. When designing both the column and the beam, the target levels y_t and μ_t corresponding to different performance levels were considered. The concrete had the following properties: (a) characteristic strength f_{cm}=30 N/mm^2; (b) maximum size of aggregate=20 mm; and (c) concrete cover =30 mm. The steel reinforcement had the following properties: (a) static yield strength f_s for longitudinal high tensile steel reinforcement (T bars)=460 N/mm^2; and (b) design yield strength (f_v) for mild yield steel (R Bars) stirrup=250 N/mm^2. In order to account for the high strain rate effects present in blast conditions, dynamic increase factors, which are equal to 1.2 for concrete and 1.3 for reinforcement, respectively, were adopted [TM5-855-1, United States Department of Army (1990) and May and Smith (1995)]. In other words, the respective dynamic strengths were approximated as a product of the static strengths and the corresponding dynamic increase factors.

The parameters of the blast load determined by a commonly used program such as CONWEP (Hyde 1991) for the RC column subjected to blast loads generated by the equivalent of 100-kg TNT at a 5-m standoff distance are tabulated in Table 1. Similarly, the parameters of the blast load for the RC beam are shown in Table 2. The design of the two RC members adopted the method based on the NES, and the designs of the RC members are summarized in Table 3. The column was designed to a level characterized by very low protection and overall structure not repairable (Ward 2004). The beam was designed to a level characterized by low protection with some elements not repairable (Ward 2004).

According to the design method described, the details of the reinforcement for the RC column are shown in Fig. 3. Similarly, the details of the reinforcement for the RC beam using the same design method are shown in Fig. 4.

Construction, Instrumentation, and Testing Arrangement

The column and the beam were cast in a vertical and horizontal position respectively. A sufficiently large foundation was designed to achieve the fixed-end boundary condition at the base of the RC column, which is characteristic of a cantilever column. The dimensions of the foundation are 2,300 by 1,400 by 500 mm, and the foundation was made in a single placement of concrete (Fig. 3). Connective steel plates were used for the RC beam to produce a pin support to the foundation block. The foundation block in this case was sufficiently large to minimize free body rotation, and the dimensions are 1,200 by 1,000 by 1,000 mm (Fig. 4). The connective steel was fabricated using 50-mm-thick plates.

In order to replicate the way that RC columns are typically cast on site, the placement of the column was undertaken in two stages. Within the first stage, the casting was undertaken from the bottom of the foundation blocks up to a level of 200 mm above the top surface of the foundation blocks. The remainder of the column was cast two days later after scouring the surface of the hardened concrete made in the previous cast. The scouring sought to roughen the surface between the concrete to be cast and the concrete already cast. The cantilever column and its foundation block are shown in Fig. 5. The simply supported beam and the connective steel plates are shown in Fig. 6.

At selected points along the height of the RC column and the length of the RC beam, pressure gauges, accelerometers, and strain gauges measured the variation of blast pressure, horizontal acceleration, and longitudinal reinforcement strain, respectively, against time. The locations of these selected points of measurement and gauges are shown in Figs. 7 and 8.

Test Results and Observations

Actual blast tests were carried out based on the setup of the cantilever RC column and simply supported beam. The blast pressures experienced by the column and beam were recorded. In addition, response such as the acceleration at certain points at each of the RC members is presented here. The damage of each member subjected to the blast loads is also discussed herein. The corresponding time histories for the displacement obtained through double integration of time histories of acceleration with respect to time coupled with digital signal processing to remove noise content are also presented and discussed. The displacement time histories are presented for the RC beam only. Bearing in mind that the specimens had earlier been designed adopting the method based on NES, the displacements of the RC members due to the blast loads are compared with the target levels associated with their designs. As such, this seeks to verify the applicability of the design method proposed earlier using the response of the RC members due to blast loads, arising from actual explosions.

Pressure due to Blast Loading

The time histories of the pressure recorded were compared with the pressure approximated by CONWEP. This comparison of pressure obtained from the RC column and beam are shown in Figs. 9 and 10, respectively. The peak blast pressures for the cantilever RC column as approximated by CONWEP at the point near the fixed end (i.e., 0.12 of the column height) are similar to those recorded from the explosion. However, due to a diffraction of the blast waves nearer to the free end (i.e., 0.53 of the column height), the peak pressures approximated are significantly larger than those recorded. Similarly, the impulses approximated by CONWEP are significantly larger than those determined from the tests. Here, the area under the time history of pressure is used as a proxy for the impulse of the blast. Therefore, using the blast parameters as determined by CONWEP can be conservative for the design of a cantilever RC column based on the pressure and impulse approximated.

A similar comparison was made between blast parameters of the RC beam as approximated by CONWEP and those recorded from the explosion tests (Fig. 9). The pressure was recorded at points 0.04 and 0.50 of the beam span as measured from the pin support. The peak blast pressure as recorded was similar to that as approximated by CONWEP for points near the pin support and at the midspan of the beam. Unlike the RC column, the peak pressure and impulse as approximated by CONWEP was not significantly more conservative than the recorded values. Along the beam, the pressure at different locations along the beam is measured at the same level above the ground since the beam was placed horizontally on the ground. On the other hand, the pressure experienced by the column varied significantly along the height of the column due to diffraction of the blast waves. This suggests that CONWEP may be more conservative in terms of approximating the blast parameters further along the height of a column, at positions further away from the ground, where the detonation was.

Observations of Blast Response

Several cracks formed near to the top of the foundation (i.e., fixed end) on the cantilever column, at a location about 200 mm from the top of the foundation (i.e., 0.07 of the column height). Fig. 11 shows these cracks near the fixed-end support. Not many diagonal cracks characteristic of flexural behavior were observed, which suggests that the behavior of the RC column was predominantly in a direct shear behavior when subjected to a blast at a short standoff distance. In terms of a design philosophy for RC columns subjected to blast loads at a short standoff distance, attaining sufficient shear capacity would be likely to mitigate the failure of the column. Another type of damage to the column consists of numerous recesses on the concrete formed by flying debris, as shown in Fig. 11. The observed extent of the recesses formed may have little consequence on its structural strength.

The damage observed on the simply supported beam is shown in Fig. 12. Along the midspan of the beam, flexural cracks formed with a spacing of about 170–220 mm. The width of the cracks was largest near the midspan, and those cracks formed away from the midspan (i.e., closer to the pin support) were finer. The width of the widest crack formed was about 2 mm wide. The length of this crack was 250 mm long, and almost traversed across the entire width of the face of the beam perpendicular to the direction of propagation of the blast wave. These cracks were formed on the back face of the beam, which refers to the face away from the incoming blast wave. On the front face, no cracks were formed. This is because as the blast wave arrived, the beam underwent deformation. During this deformation which is predominantly flexural in nature, the front face experiences compression while the back face experiences tension.

Displacement Response

There were only two accelerometers installed on each specimen to measure their dynamic responses due to the limited availability of channels of the data acquisition system used during the tests. Therefore in order to obtain the displacement response, integration of acceleration is necessary. There is noise content present within the recorded acceleration data, and so a direct double integration of the acceleration time histories, with respect to time, is not appropriate in determining the time histories of displacement. Thus, the method proposed by Su (1998) was used to determine the time histories of displacement.

For the beam, the acceleration and displacement for two locations on the beam is discussed, which are as follows: (a) a point near to the pin support and (b) at the midspan of the beam. The beam was designed with a target level of 75 mm at the midspan while the displacement under the blast was determined as 60 mm, which is well within the target level earlier ascertained (Fig. 13). As such, by designing the beam using the method based on NES, the beam did not experience a displacement that was larger than the level it was designed for. It shows that the design method based on NES provides a sufficient design as verified by actual explosion tests. It can be seen that the displacement near to the pin support is small compared to that at the midspan. For the beam tested within this paper, the beam behaves mainly in flexural bending.

In the beam, the target level adopted by the design is significantly larger than that experienced by the members, and can be deemed to be rather conservative. There may be two possible reasons for this. First, the approximation of the blast parameters by a program such as CONWEP may be conservative. This was demonstrated by the comparison of the approximated peak pressure with the recorded peak pressure. Second, approximating the mechanical properties of a homogeneous material such as RC has always been a challenge and some level of conservatism may exist. Nevertheless, the design method based on NES proved to be more conservative in the case of the column than the beam.

Reinforcement Strain Response

The strains of longitudinal reinforcement bars within the column and the beam are shown in Figs. 14 and 15, respectively. For the column, the strain was recorded near the fixed-end support. As for the beam, the strain was recorded on both faces of the beam which refers to the face nearer to the source of explosion (i.e., compression) and the face away from the source of explosion (i.e., tension face). The peak strain experienced was largest in the longitudinal rebar of the column near the fixed-end support with a value of about 2.5 microstrains. For the longitudinal rebars at the midspan of the beam, both tensile and compressive strains had a peak value of about 3.5 microstrains. Further inspection of the time histories of the strain show a peak at the early stages of loading and then decrease to a lower mean value over time. It can be seen that the design of the beam and column using the method based on NES was adequate for the blast scenario of short standoff distance. The design in terms of cross-sectional area and amount of steel reinforcement was sufficient such that the displacement was not sufficiently high that the rebar would experience a sustained level of high strain. This also adds to demonstrating that the design of the RC members using the method based on NES is viable for the design of RC beams for a blast scenario of short standoff distance.

Conclusions

This paper set out to verify an earlier proposed method for the design of RC members to blast loads, based on NES. To do this, explosion tests were conducted on a RC column and beam, which had been designed using the method. Here, the paper is limited to the study of RC members subjected to blast loads at a short standoff distance. Comparisons were made between the responses due to the blasts and the target levels of response which the members had been designed for. Observations were also made on the behavior of the members due to the blast load. Limited to this study, the conclusions are as follows:

1. When subjected to the blast load at a short standoff distance, the cantilever column

behaved predominantly in direct shear. As such, ways of mitigating the damage of a cantilever column, subjected to a blast scenario characterized by a short standoff distance, should be aimed at improving its direct shear capacity (i.e., robustness).

2. From the blast loadings recorded in the test, the blast pressure calculated by CONWEP possesses enough accuracy for engineering purposes if there is no significant diffraction of the blast waves around the member. Otherwise the real blast pressure will be significantly smaller than the calculated value.
3. The design method based on NES provides a feasible design for the blast resistant design of members, subjected to blast loads at a short standoff distance. The method may be conservative such that the response of the member may be lower than the target level at which it was designed for.

Acknowledgments

This research was supported by a research grant provided by the Defense Science and Technology Agency (DSTA), Singapore under the Protective Technology Research Center, Nanyang Technological University, Singapore. Any opinions, findings and conclusions expressed in this paper are those of the writers and do not necessarily reflect the view of DSTA, Singapore.

Appendix. Determining Displacement from Recorded Acceleration

The acceleration response was recorded from actual blast tests. The displacement response was then numerically derived from recorded acceleration response. This section describes the method used to determine the time histories of displacement from the time histories of acceleration by numerical means. As there is noise content present in the recorded acceleration signals, a direct double integration of the acceleration signals, with respect to time, is not appropriate in determining the time histories of displacement. Some level of digital signal processing is required in conjunction with the double integration of acceleration signals with respect to time. It was found that a constant component in the time history of velocity could not be effectively removed (Toussi and Yao 1983). Another method was proposed by Su (1998) whereby the steps are summarized as follows:

1. Use a smoothing process to remove the high frequency components within the time history of acceleration to generate a new time history of acceleration;
2. Integrate the new time history of acceleration to determine the time history of velocity;
3. Perform a curve fitting of the time history of velocity generated by Step 2, with a fifth-order polynomial using an optimum searching algorithm to arrive at a secondary time history of velocity;
4. Remove the secondary time history of velocity from the time history of velocity generated by Step 3, to arrive at a tertiary time history of velocity; and
5. Finally, integrate the tertiary time history of velocity to obtain the time history of displacement.

This method has proved effective in determining the time history of displacement from a recorded time history of acceleration. However it should be pointed out that the results of this method are only credible when the signal-noise ratio of the response is sufficiently large (Chiu 1997).

References

Allgood, J. R., and Swihart, G. R. (1970). “Design of flexural members for static and blast loadings.” *American Concrete Institute Monograph Series, No. 5*, Detroit, 147–149.

ASCE. (1985). “Design of structures to resist nuclear weapons effects.” *Manual 42*, New York.

Biggs, J. M. (1964). *Introduction to structural dynamics*, McGraw-Hill, New York.

Chiu, H. C. (1997). “Stable baseline correction of digital strong-motion data.” *Bull. Seismol. Soc. Am.*, 87, 932–944.

Corley, W. G., Mlakar, P. F., Sozen, M. A., and Thornton, C. H. (1998). “The Oklahoma City bombing: Summary and recommendation for multi-hazard mitigation.” *J. Perform. Constr. Facil.*, 12(3), 100–112.

Hayes, J. R., Woodson, S. C., Pekelnicky, R. G., Poland, C. D., Coley, W. G., and Sozen, M. (2005). “Can strengthening for earthquake improved blast and progressive collapse resistance?” *J. Struct. Eng.*, 131(8), 1157–1177.

Hinman, E. E., and Hammond, D. J. (1997). *Lessons from the Oklahoma City bombing: Defensive design techniques*, ASCE, New York.

Hyde, D. W. (1991). “ConWep: Weapon effects calculation program based on technique manual, TM5-855-1.” United States Army Engineer Waterways Experiment Station.

Li, B., Pan, T.-C., and Nair, A. (2009). “A case study of the local and global structural responses of a tall building in Singapore subjected to close-in detonations.” *The structural design of tall and special buildings*, published online July 19, 2009.

Longinow, A., and Mnizsweski, K. R. (1996). “Protective building against vehicle bomb attacks.” *Pract. Period. Struct. Des. Constr.*, 1(1), 51–54.

Luccioni, B. M., Ambrosini, R. D., and Danesi, R. F. (2004). “Analysis of building collapse under blast loads.” *Eng. Struct.*, 26(1), 63–71.

May, G. C., and Smith, P. D. (1995). *Blast effect on building: Design of buildings to optimize resistance to blast loading*, Thomas Telford, London.

Mlakar, P. F., Corley, W. G., Sozen, M. A., and Thornton, C. H. (1998). “The Oklahoma City bombing: Analysis of blast damage to the Murrah building: Investigation of the bombing of the Oklahoma City federal building." *J. Perform. Constr. Facil.*, 12(3), 113–119.

Rong, H.-C., and Li, B. (2008). "Deformation-controlled design of reinforced concrete flexural members subjected to blast loadings." *J. Struct. Eng.*, 134(10), 1598–1610.

Su, X. Z. (1998). *Seismic design of prestressed concrete moment-resisting frame,* Sci-Tech Publishing House, Shanghai.

Toussi, S., and Yao, J. T. P. (1983). "Hysteresis identification of existing structures." *J. Eng. Mech.*, 109(5), 1189–1202.

United States Department of Army. (1965). "Fundamental of protective design (non-nuclear)." *TM5-855-1*, Washington, D.C.

United States Department of Army. (1990). "Structures to resist the effects of accidental explosions. Volume 4: Reinforced concrete design." *TM5-1300*, Washington, D.C.

Ward, S. P. (2004). "Retrofitting existing masonry buildings to resist explosions." *J. Perform. Constr. Facil.*, 18(2), 95–99.

List of Tables

List of Figures

Fig. 10 Time histories of pressure recorded and approximated for beam: (a) at a point 0.04 of the beam span from the pin support; (b) at a point 0.50 of the beam span from the pin support

Fig. 11 Cracks and fragments on column: (a) side view of the damaged specimen; (b) front view of the damaged specimen; and (c) fragment on the front face of the column

Fig. 12 Cracks on beam: (a) cracks observed near the midspan; (b) cracks observed near the support

Fig. 13 Acceleration and displacement responses for beam: (a) acceleration at 0.10 of the beam span from the pin support; (b) displacement at a point 0.10 of the beam span from the pin support; (c) acceleration at a point 0.50 of the beam span from the pin support; and (d) displacement at a point 0.50 of the beam span from the pin support

Fig. 14 Tension strain of longitudinal reinforcement in the column

Fig. 15 Strain history of longitudinal reinforcement in the beam: (a) tension strain history; (b) compression strain history

Blast parameters	Point 1	Point 2	Point 3
P_r (kPa)	6,650	4,350	3,730
t_d (ms)	9.29	10.09	
I_s (kPa·ms)	3,720	2,850	2,600

Table 1

Blast parameters	Point 1	Point 2
P_r (kPa)	3,980	3,050
t_d (ms)	10.28	10.26
I_s (kPa·ms)	2,930	2,520

Table 2

	Design parameters					Design results				Actual reinforcement	
Member	y_t	μ_t	f_{dc}	f_{ds}	f_{dv}	d	ρ_h (%)	ρ_v (%)	A_s (mm^2)	Rebars	Area
C1	200	10	36	59.8	32.5	260	1.02	0.24	1,176	6T16	1,205
B1	75	6	36	59.8	32.5	290	0.81	0.15	701	2T16+T20	716

Table 3

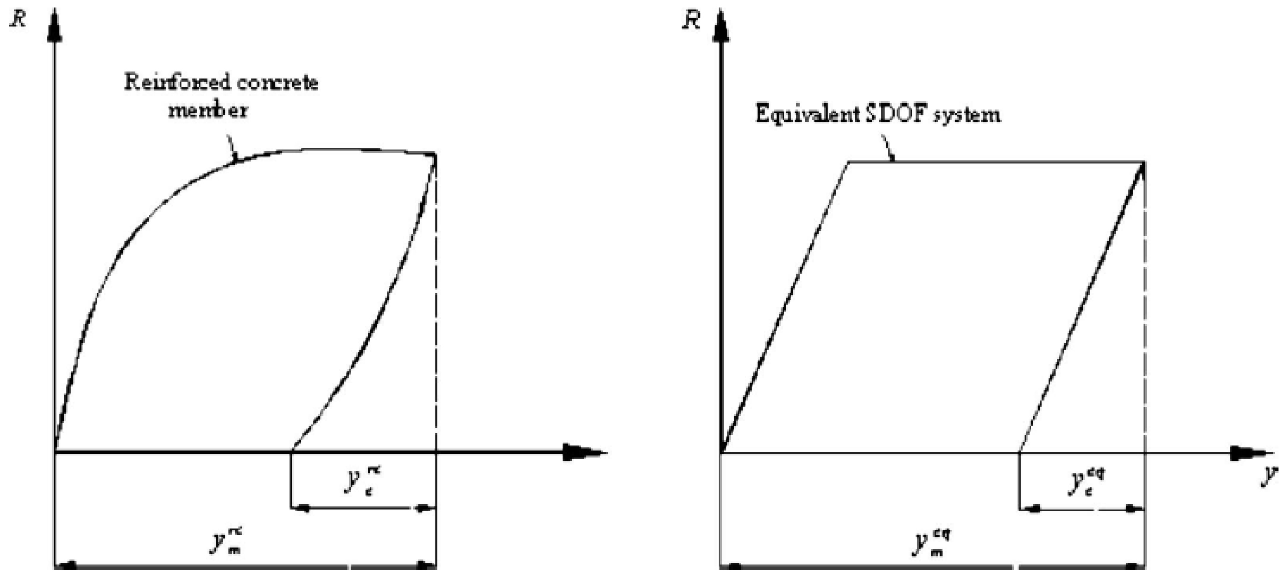

R
Reinforced concrete member
y_e^rc
y_m^rc
R
Equivalent SDOF system
y
y_e^eq
y_m^eq

Fig. 1

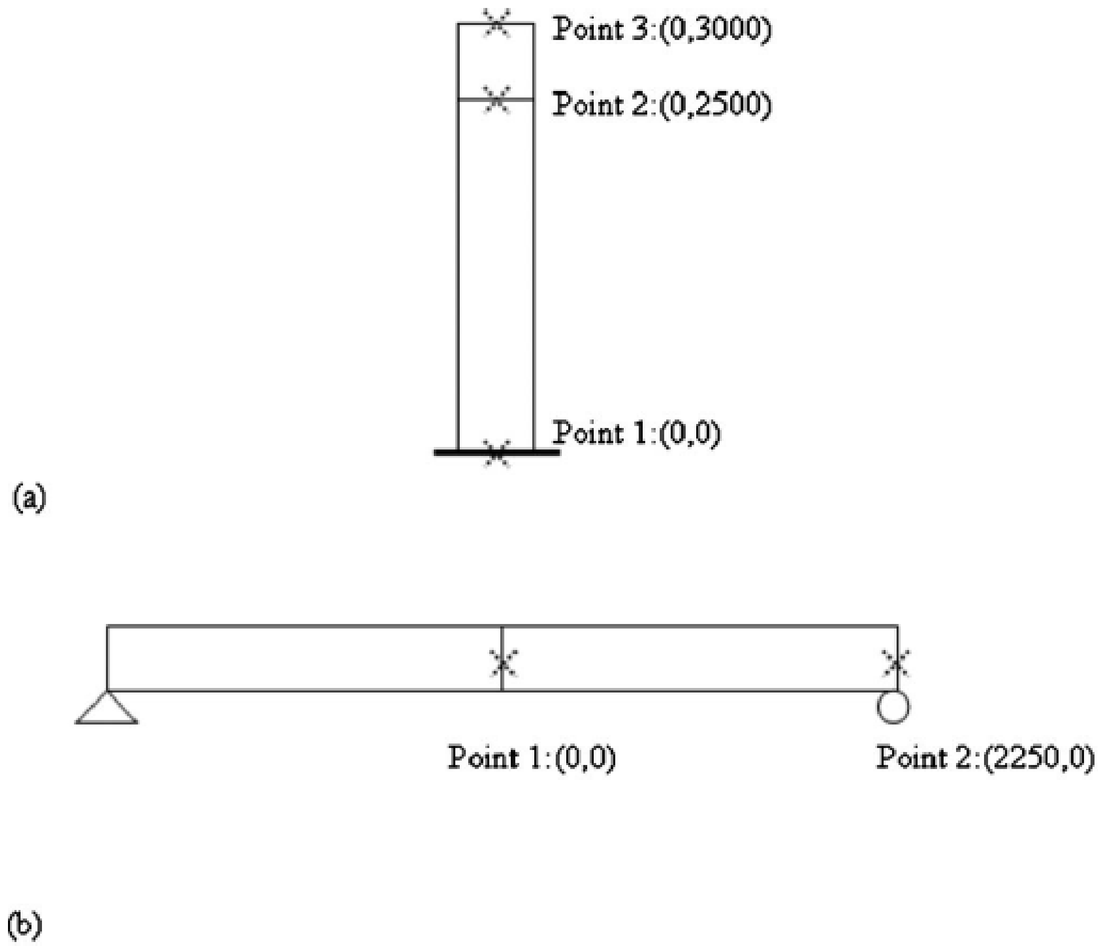
Point 3:(0,3000)
Point 2:(0,2500)
Point 1:(0,0)
(a)
Point 1:(0,0)
Point 2:(2250,0)
(b)

Fig. 2

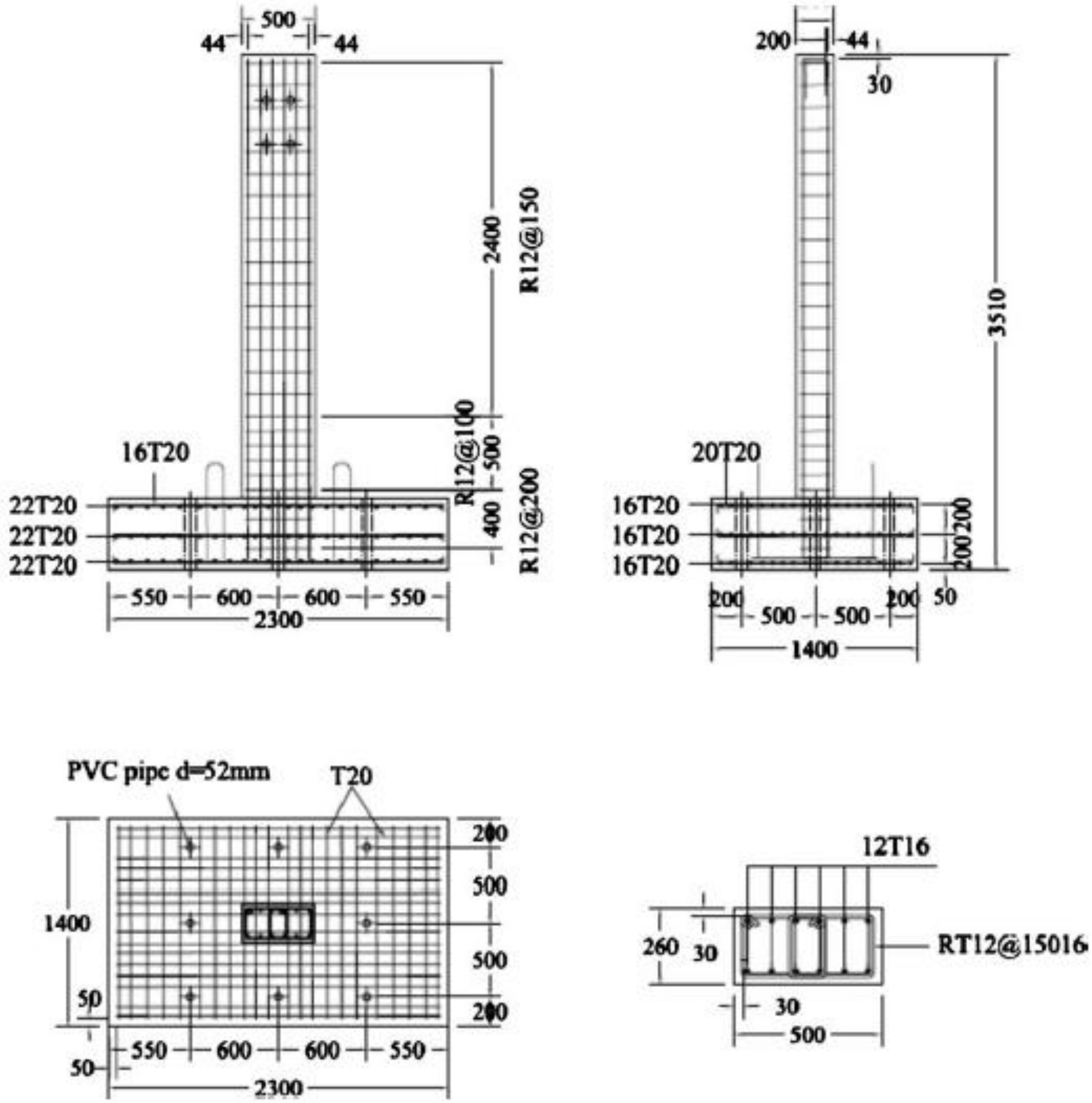
500
44
44
2400
R12@150
R12@100
500
R12@200
400
16T20
22T20
22T20
22T20
550
600
600
550
2300
200
44
30
3510
20T20
16T20
16T20
16T20
200
200
50
200
200
500
500
1400
PVC pipe d=52mm
T20
1400
200
500
500
200
50
50
550
600
600
550
2300
12T16
260
30
RT12@15016
30
500

Fig. 3

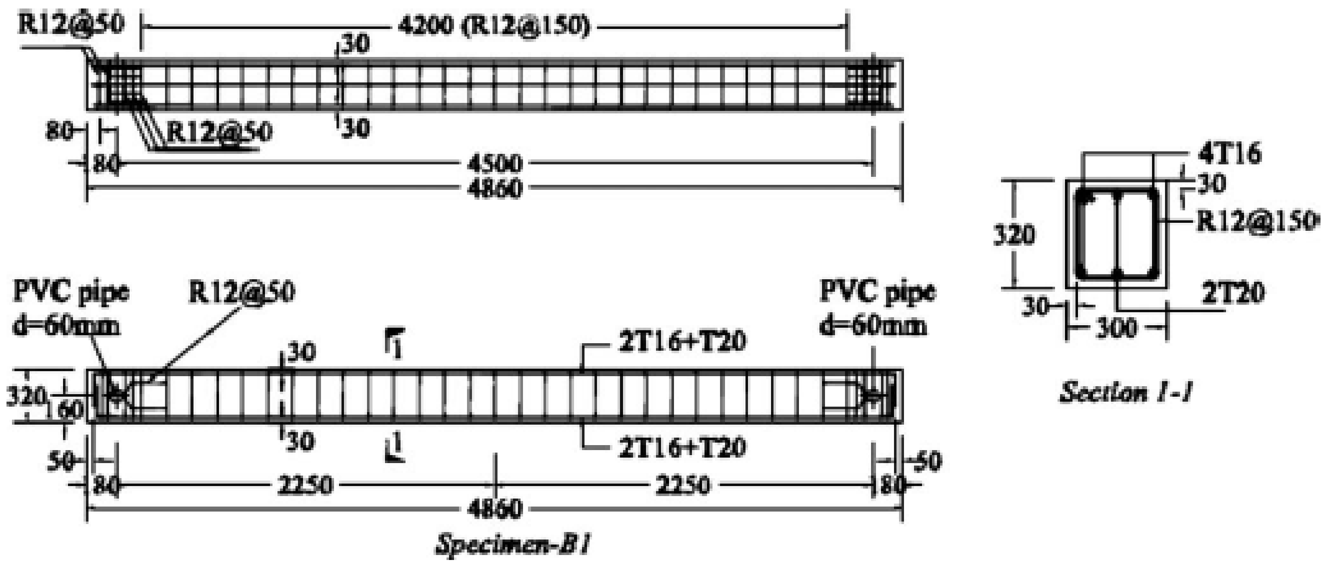
R12@50
4200 (R12@150)
30
30
80
R12@50
80
4500
4860
4T16
30
320
R12@150
30
300
2T20
Section 1-1
PVC pipe
d=60mm
R12@50
30
1
2T16+T20
PVC pipe
d=60mm
320
60
30
1
2T16+T20
50
80
2250
2250
80
50
4860
Specimen-B1

Fig. 4

(a)

(b)

Fig. 5

(a)

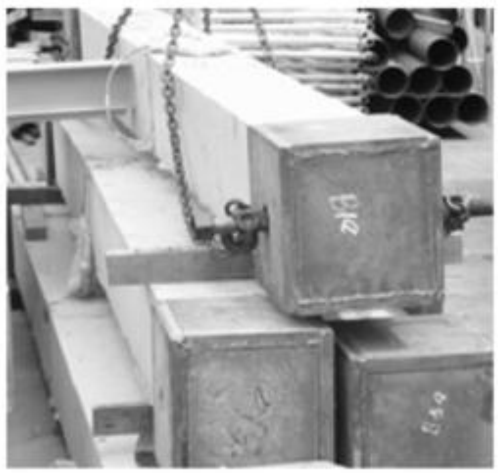

(b)

Fig. 6

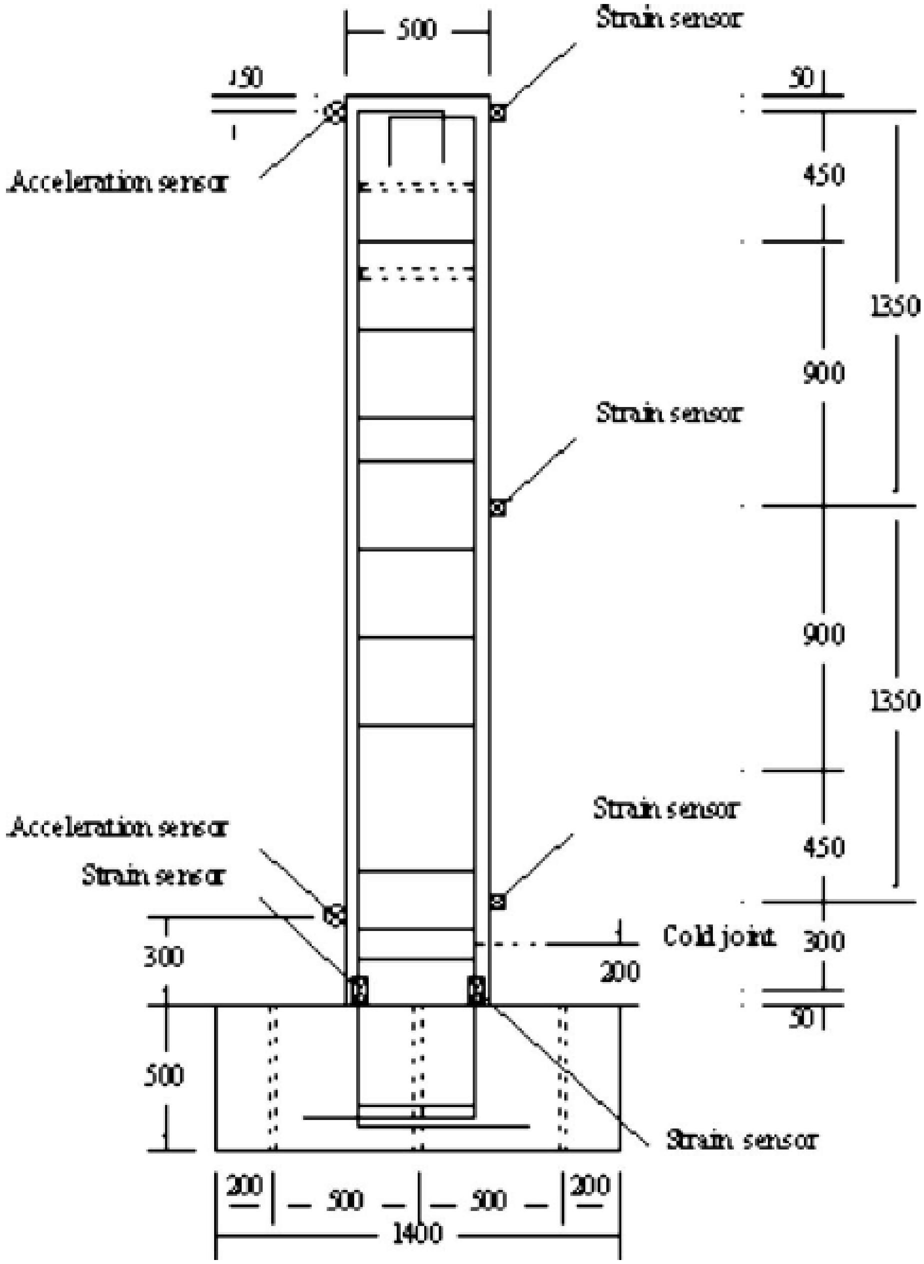

500
Strain sensor
150
50
Acceleration sensor
450
1350
900
Strain sensor
900
1350
Strain sensor
Acceleration sensor
Strain sensor
450
300
Cold joint
300
200
500
50
Strain sensor
200
500
500
200
1400

Fig. 7

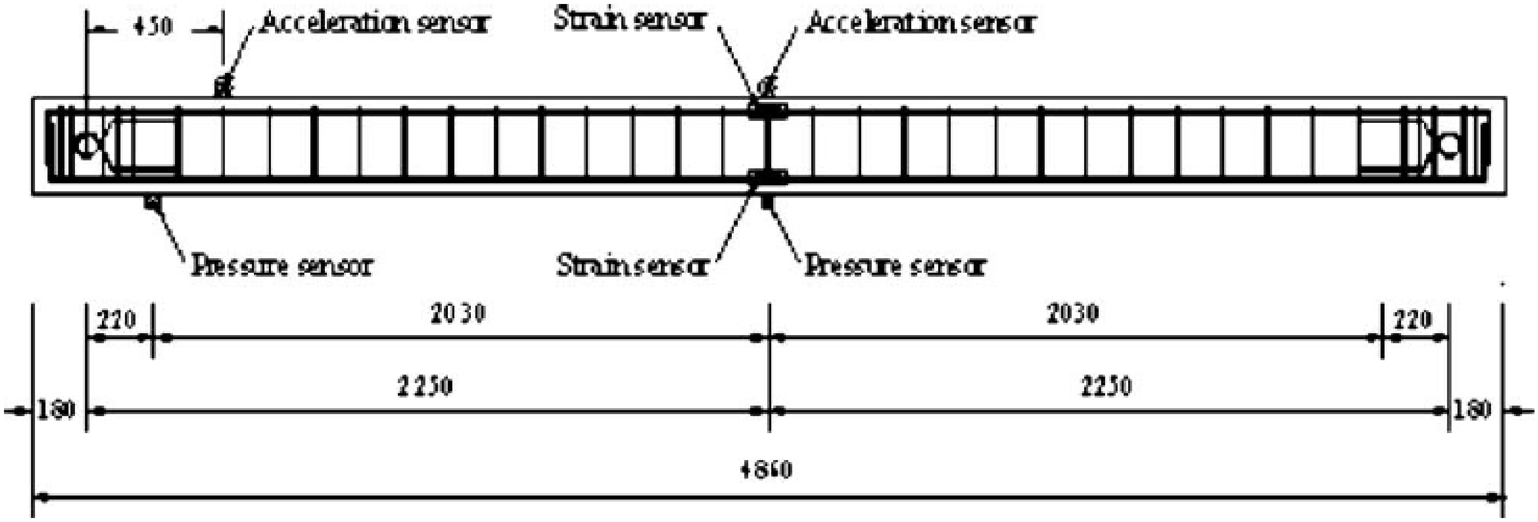
450
Acceleration sensor
Strain sensor
Acceleration sensor
Pressure sensor
Strain sensor
Pressure sensor
220
2030
2030
220
180
2250
2250
180
4860

Fig. 8

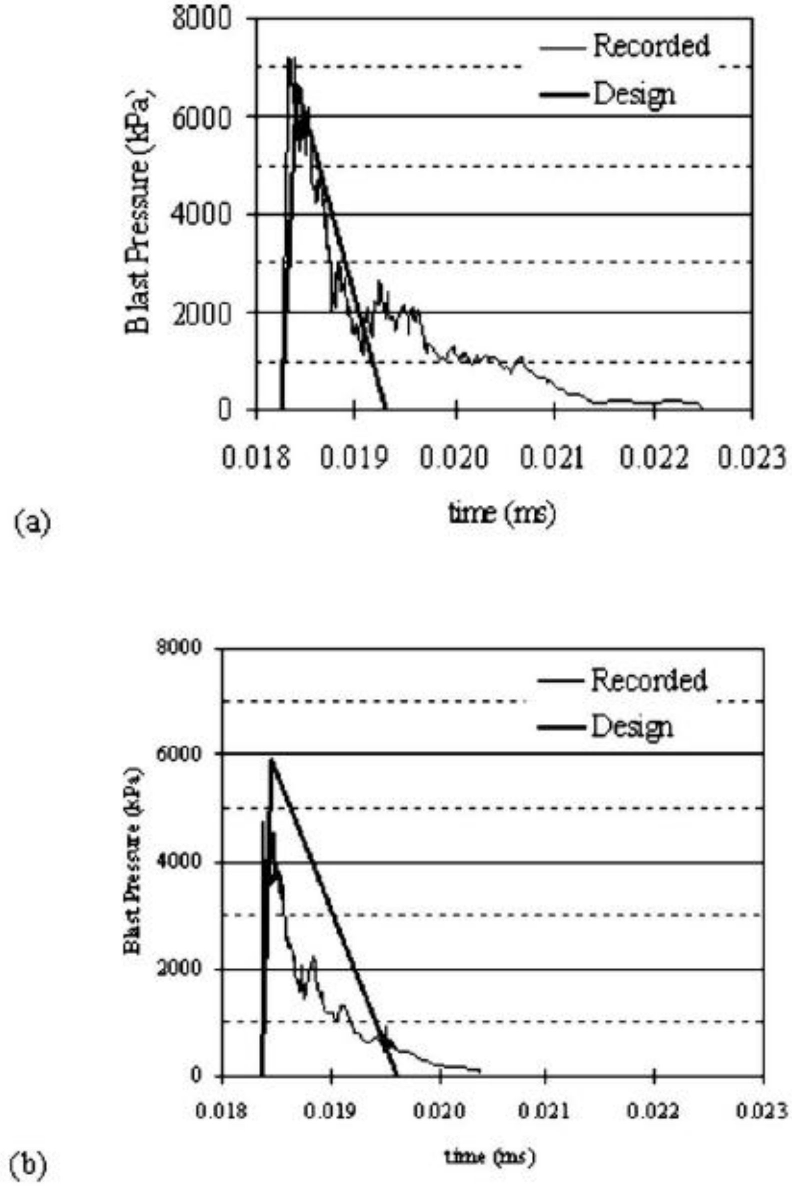
8000
6000
4000
2000
0
Blast Pressure (kPa)
Recorded
Design
0.018
0.019
0.020
0.021
0.022
0.023
time (ms)
(a)
8000
6000
4000
2000
0
Blast Pressure (kPa)
Recorded
Design
0.018
0.019
0.020
0.021
0.022
0.023
time (ms)
(b)

Fig. 9

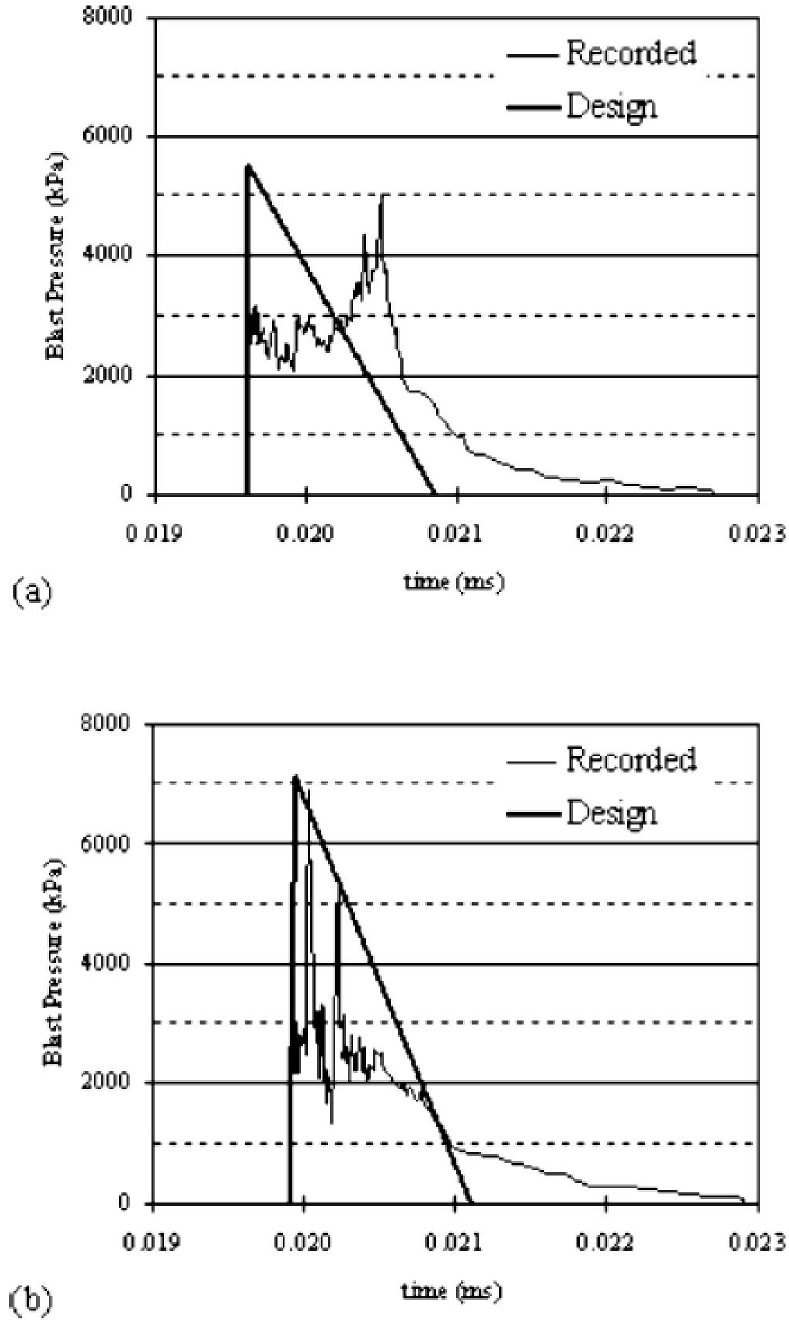
8000
6000
4000
2000
0
Blast Pressure (kPa)
Recorded
Design
0.019
0.020
0.021
0.022
0.023
time (ms)
(a)
8000
6000
4000
2000
0
Blast Pressure (kPa)
Recorded
Design
0.019
0.020
0.021
0.022
0.023
time (ms)
(b)

Fig. 10

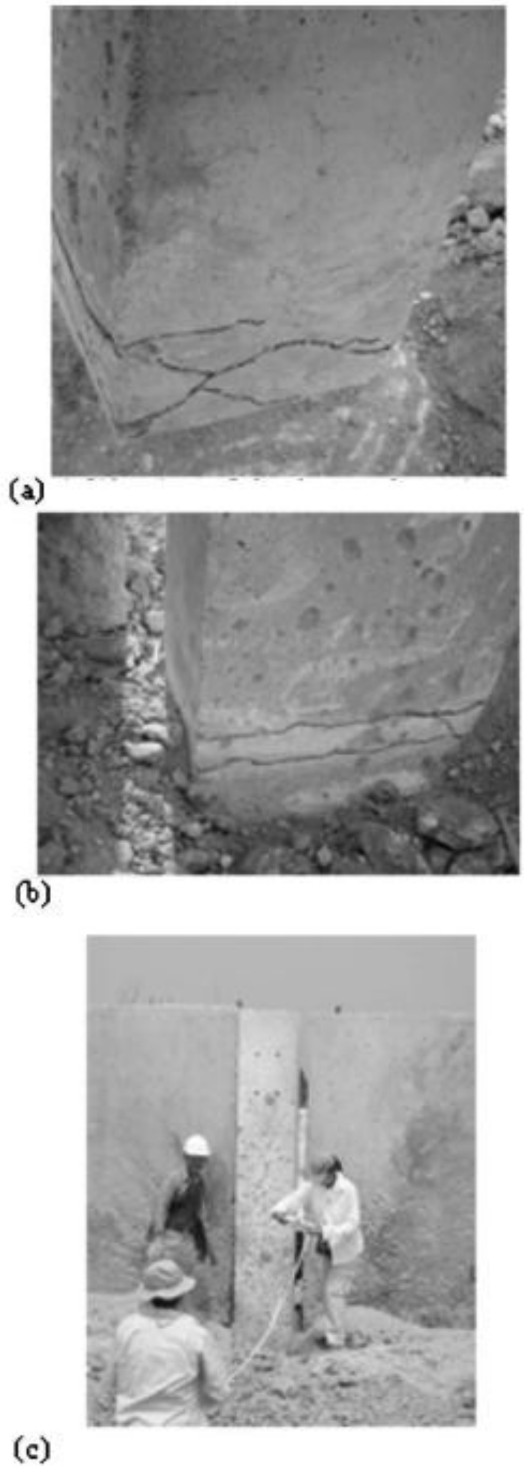

Fig. 11

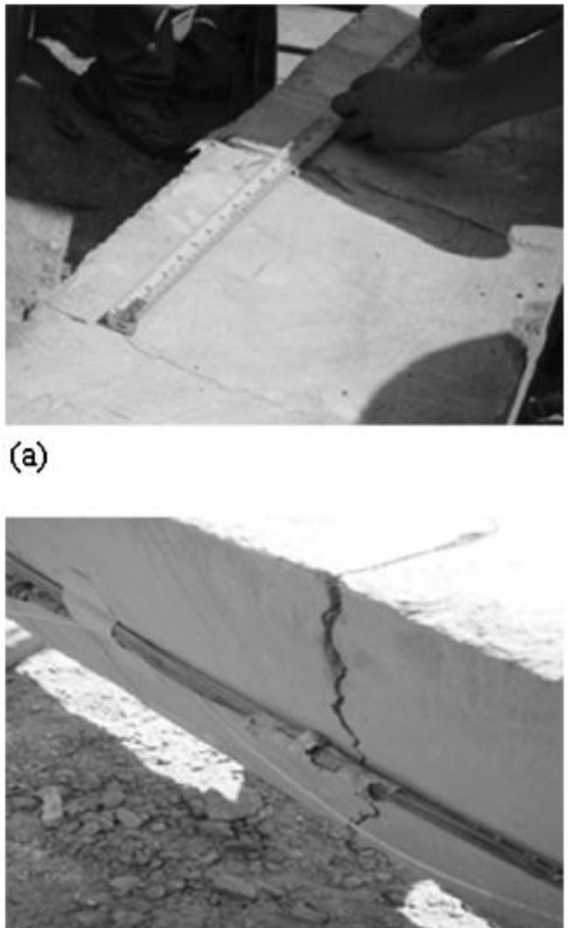

(a) (b)

Fig. 12

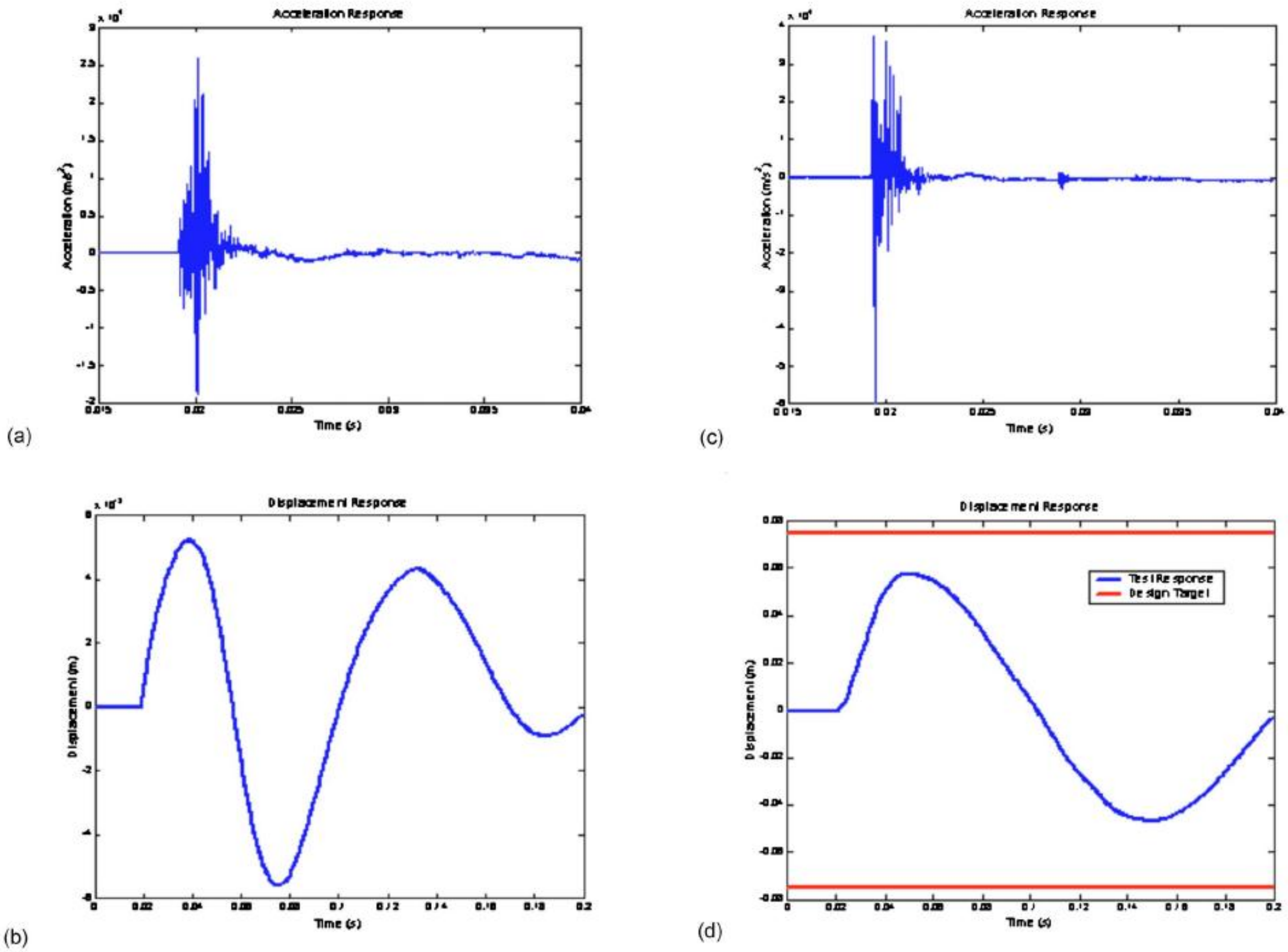
Acceleration Response
Time (s)
(a)
(c)
Displacement Response
Time (s)
Test Response
Design Target
(b)
(d)

Fig. 13

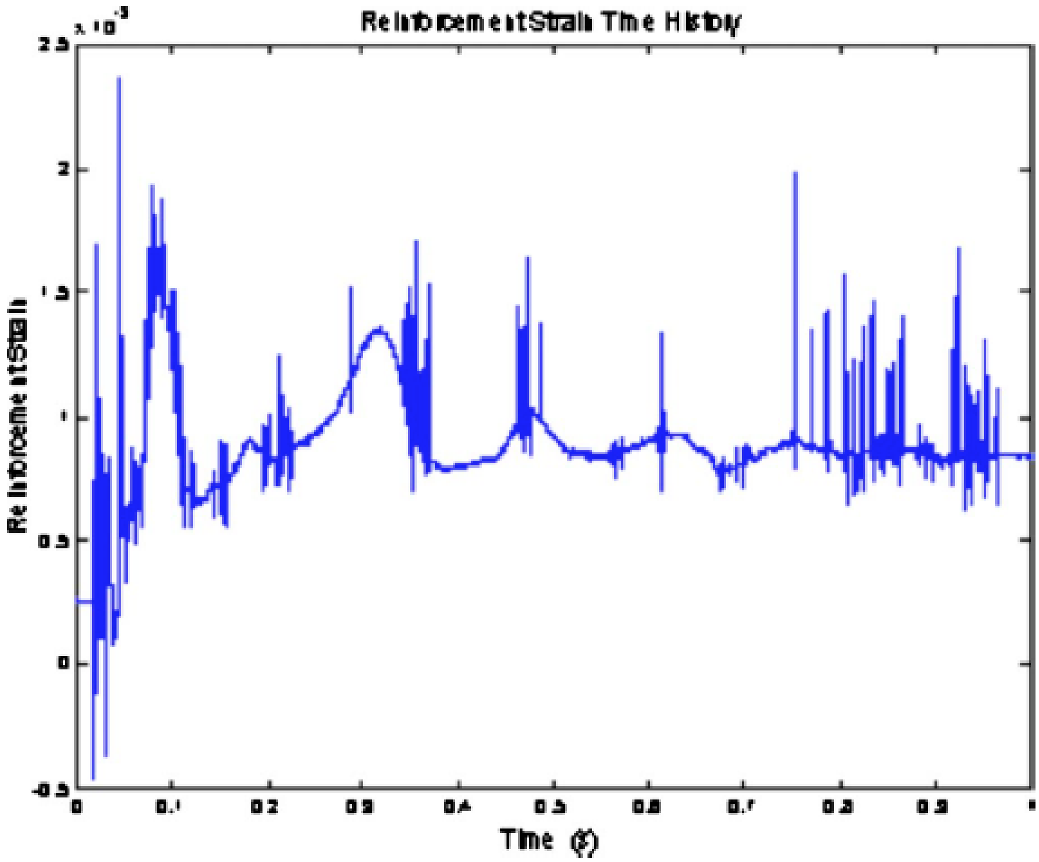
Reinforcement Strain Time History
Reinforcement Strain
Time (s)

Fig. 14

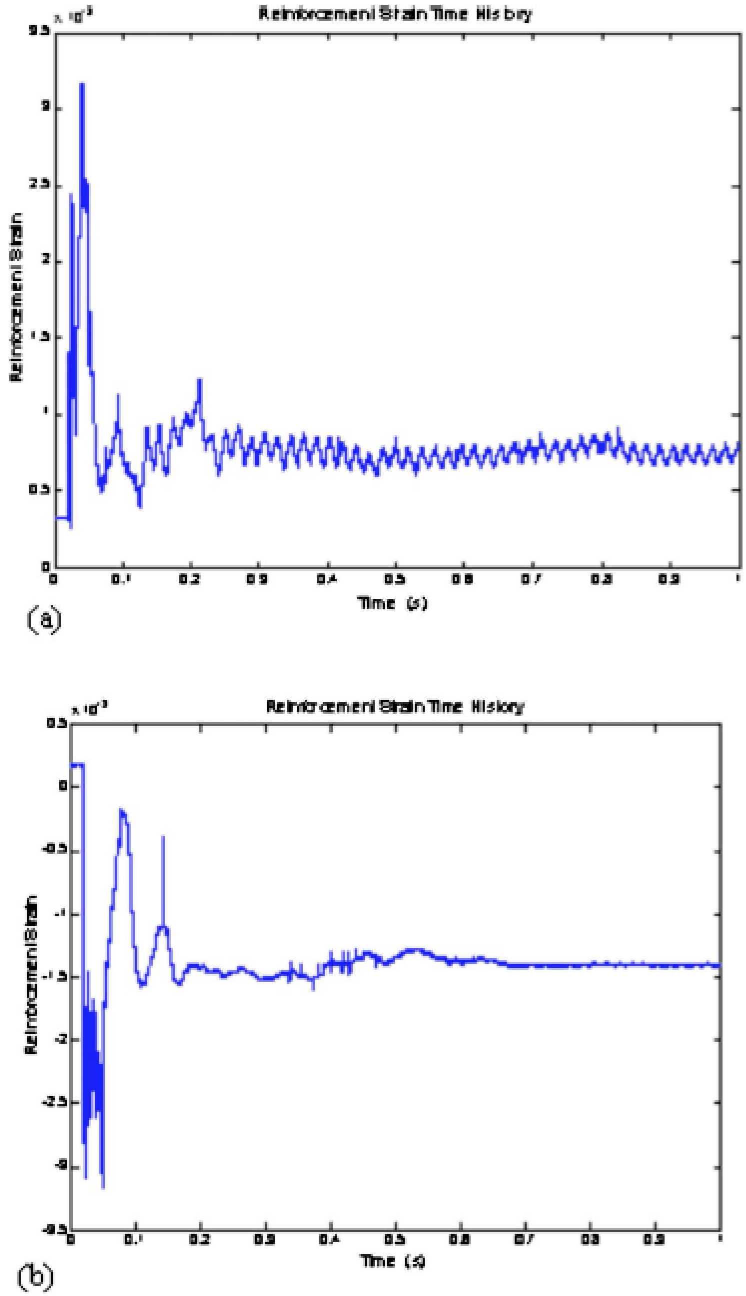
Reinforcement Strain Time History
Reinforcement Strain
Time (s)
(a)
Reinforcement Strain Time History
Reinforcement Strain
Time (s)
(b)

Fig. 15